Manufacturing of Microfibrillated Cellulose from Never-Dried Microcrystalline Cellulose Using Masuko Grinder

Annina Lähdeniemi,[a,]* Aaro Knuts,[b] and Olli Dahl [a]

Microfibrillated cellulose (MFC) batches were produced using never-dried and commercial, dried microcrystalline cellulose (MCC) as raw materials. Mechanical treatment was applied with a Masuko grinder using different refining degrees and consisting of one to three passes through the equipment. The impact of the mechanical treatment on the particle size distribution, fiber swelling properties, particle morphology as well as rheology of the manufactured MFC gel products were investigated. In addition, specific energy consumption of the process was calculated. The MFC gel samples manufactured from the never-dried AaltoCell™ MCC, demonstrated more pronounced changes in material properties with various refining parameters than those produced from the commercial, dried MCC, which is likely attributable to the hornification effect. The most significant reduction in particle sizes and the greatest increase in fiber saturation point and rheological properties were achieved during the initial pass through the grinder. The use of never-dried MCC as the raw material resulted in a stronger MFC gel with higher storage and loss modulus characteristics. Specific energy consumption also indicated that the refining energy transfers better to the never-dried structure of MCC, and more fibrillation can be obtained with less energy when using the never-dried MCC as raw material for MFC production.

DOI: 10.15376/biores.19.4.9375-9395

Keywords: Microcrystalline cellulose; MCC; Cellulose mechanical treatment; Masuko grinder; Microfibrillated cellulose; Cellulose hydrogel; Never-dried MCC; MFC production

*Contact information: a: Department of Bioproducts and Biosystems, Aalto University School of Chemical Technology, PO Box 16300, Vuorimiehentie 1, Espoo, Finland; b: Scitech Oy, Eteläesplanadi 22, 00100 Helsinki, Finland; *Corresponding author: annina.lahdeniemi@aalto.fi*

INTRODUCTION

Microfibrillated cellulose (MFC), also referred sometimes to as nanocellulose, is one of the most promising innovations for the forest sector. Microfibrillated celluloses consist of microfibril bundles with diameters predominantly in the range of 10 to 100 nm forming a weblike fibrillar network. Within the last decades, MFCs have gained much attention for their promising utilization in composites, coatings, and films due to their large specific surface areas and unique mechanical properties. Outside the forest industries, micro- and nano-cellulosic products have already been used in various other industries in high-value applications, such as cosmetics, pharmaceuticals, and food ingredients because of their renewability, low cost, biodegradability, low toxicity, and good biocompatibility. A hydrolyzed, microcrystalline cellulose (MCC) that is in the form of pure cellulose, has earlier been granted the E-number E460 by the European Food Safety Authority.

Microfibrillated cellulose was first produced in 1983 by Turbak *et al.* (1983) using wood pulp and a high-pressure homogenizer, which promoted the disintegration of cellulosic fibers into substructural fibrils and microfibrils having lengths in the micron scale and widths ranging from 10 to a few hundred nanometers. This material was found to form stable aqueous suspensions, providing an opportunity for multiple uses as thickeners, emulsifiers or additives in food, paints, and coatings, as well as cosmetics and medical products. The MFCs have impressive mechanical properties, thus making the material ideal as a reinforcement in composites and, concurrently, to reduce the utilization of petroleum-based components.

Mechanical approaches to diminish cellulosic fibers into nano- or micro-scale can be divided into refining and homogenizing, microfluidization, grinding, cryo-crushing, and high intensity ultrasonication (Khalid *et al.* 2014). Devices such as high-pressure homogenizer (HPH), Valley beater (laboratory Hollander), microfluidizer, ball mill, Masuko grinder, aqueous counter collision (ACC), and rotor stator cavitron have been tested in the past (Manninen *et al.* 2011; Ankerfors 2012; Guezennec 2012; Ardanuy *et al.* 2012; Kondo *et al.* 2014; Zhang *et al.* 2015; Taheri and Samyn 2016). In general, mechanical processing produces high shear that causes transverse cleavage along the longitudinal axis of the cellulose microfibrillar structure, resulting in the extraction of long cellulose fibrils. The size reduction of cellulosic chains occurs due to the increased mechanical damage to the crystalline cellulose, which can be observed by the decline in crystallinity (Moon *et al.* 2011; Lengkowski *et al.* 2018). All in all, mechanical processing creates more surface area, more open structure, and to lower portion of less reactive crystalline region of cellulose.

Much energy is generally required to produce MFC. Different mechanical MFC production methods consume energy at different levels. Consequently, the energy consumption during production is an important aspect in the determination of the “green” nature of these MFC-based materials. Previous research has mainly focused on chemical pretreatments such as enzymatic hydrolysis (Henriksson *et al.* 2007) and TEMPO-mediated oxidation (Saito and Isogai 2004) for reducing energy consumption in the MFC process.

MFC generally is produced by fibrillating the fibers under high compression and shear forces. Cellulose fibrils in plant cell walls are, however, tightly hooked to one another by multiple hydrogen bonds; thus, it is difficult to individualize cellulose fibrils only by short mechanical treatment. Therefore, it is favorable to reduce the size of the fibers before their passing through the equipment (Khalid *et al.* 2014). Hence, MCC consisting of bundles of crystallites with different particles has attracted attention as a promising raw material for MFC production. MCC particles can immobilize high amounts of water on both the external and internal surfaces, which is accompanied by the formation of gel-like water systems (Ioelovich and Leykin 2008).

A grit-like plate grinder, the Masuko Supermass Colloider, has a proven ability to influence an already micro-size cellulose material. Moreover, the Masuko grinder has been widely used in numerous research regarding MFC production with different raw materials and pre-treatments (Taniguchi and Okamura 1998; Uetani and Yano 2011; Josset *et al.* 2014; Lahtinen *et al.* 2014). In general, the grit-like filling of the Masuko grinder has smaller channels for fibers to pass through in the energy dissipating zone and thereafter higher “impact rate” compared to the traditional steel-bar fillings. The principle of the grinding phenomena is to transfer the energy from the rotating special grit-type filling to the material to have a fibrillation effect. The Masuko has been known to generate low internal fibrillation but high external fibrillation (Wang 2006). The mechanism of fibrillation in the grinder is to break down hydrogen bond and cell wall structures by shear forces and individualization of fibers to micro- and nano-scale (Siro and Plackett 2010).

In most of the MCC/MFC related studies, the raw material has been dried MCC, since it has been the only commercially available class of MCC product. For this reason, the difference in the properties of the MFCs manufactured from different MCC-types is not clear or much researched. It is well-established knowledge that drying has a permanent effect on the structure of kraft fibers. Upon the drying of cellulose, the formation of internal hydrogen bonds between cellulose fibrils makes a secondary separation into single fibrils more difficult, a phenomenon that is commonly known as hornification (Spence *et al.* 2010). Hornification leads to decreased fiber swelling capacity and stiffer fibers, leading to a cellulose material with a poorer water holding capability, poorer beat ability and reduced strength properties (Stone *et al.* 1968; Hubbe *et al.* 2007; Brancato 2008; Eriksen *et al.* 2008; Song and Law 2010; Spence *et al.* 2010; Letková *et al.* 2011). Because the never-dried MCC does not require the expensive drying step after the acidic hydrolysis manufacturing process, it is more economical to produce or purchase than the dried MCC.

Only a few previous studies can be found of the use of never-dried raw material in MFC/NFC production. Iwamoto *et al.* (2008) suggested the use of never-dried source materials to facilitate the fibrillation process. Ioelovich and Leykin (2008) reported that the HPH-processed dispersions containing never-dried MCC particles had larger internal specific surface values and higher amounts of retained water compared to those with traditional dried MCC. Ioelovich also discovered that the drying of MCC decreases both the particles' internal surface and the viscosity of the HPH-manufactured gel dispersions. These effects were explained by the irreversible closing of the internal MCC pores. Vanhatalo *et al.* (2016) used never-dried MCC raw material in high-pressure fluidization. They found that differences in MFC suspension gel strengths were straightly linked to the drying history of the MCC-materials. Thus, with never-dried MCC raw material it is possible to produce MFC with high gel strength properties. In the best knowledge of authors, no research of grinding a never-dried MCC into MFC has been reported before.

In this study, unmodified, never-dried MCC (AaltoCell™) was investigated as a raw material in the mechanical Masuko-grinding process using different grinding loads and rotation rates in order to produce MFC gels. The main aim was to discover a simple and energy efficient method for manufacturing MFCs without any additives, and to investigate the effects of the altering mechanical treatment levels on the particle morphology, the particle size distribution, fiber swelling properties, and rheology of the manufactured MFC gel products as well as the process energy consumption.

EXPERIMENTAL

Production of Never-dried MCC (AaltoCell™)

The never-dried cellulose raw material used was MCC manufactured with the AaltoCell™ method, as described in Vanhatalo and Dahl (2014). In brief, bleached softwood kraft pulp was hydrolyzed with a 1.5 % dosage of sulfuric acid at 160 °C in 10 % consistency for 110 min using tube like reactor with volume of 2.5 dm^3. After the hydrolysis, the reactor was cooled, and the MCC material was washed with distilled water in a Büchner funnel until the washed filtrate conductivity was below 5.0 µS. The washed MCC material was centrifuged at 4500 rpm with a filter bag to the dry consistency of 45%.

The yield of AaltoCell MCC was 90% (relative to the starting dry mass of the kraft pulp) and molecular weight 156.8 kg/mol.

Production of the MFCs with Masuko Grinder

Two different raw materials were used for MFC production: commercial dried MCC from wood pulp by JRS Pharma and never-dried AaltoCell™ MCC. Both MCCs were diluted with distilled water to the consistency of 10%. Two different grinding power levels (2 and 3 kW) and rotation rates (1700 rpm and 2200 rpm) were used to examine the effect of the grinding parameters on the processed MFC. Processing pressure in the Masuko grinder was 1.0 bar with the frequency of 35 Hz, and the cellulose-water slurry temperature was kept under 80 °C during processing. Samples were collected after 1, 2, and 3 grinding passes and stored at 4 °C. Produced test points and their features are presented in Table 1.

Table 1. Produced MFC Test Points and the Used Grinding Parameters

Test Point	Raw Material	Passes	Grinding Power (W)	Rotation Rate (rpm)
AC 1	AaltoCell	1	2000	1700
AC 2	AaltoCell	1	2000	2200
AC 3	AaltoCell	1	3000	1700
AC 4	AaltoCell	1	3000	2200
JRS 1	JRS Pharma	1	2000	1700
JRS 2	JRS Pharma	1	2000	2200
JRS 3	JRS Pharma	1	3000	1700
JRS 4	JRS Pharma	1	3000	2200
AC 5	AaltoCell	2	2000	2200
AC 6	AaltoCell	3	2000	2200
AC 7	AaltoCell	2	3000	2200
AC 8	AaltoCell	3	3000	2200
JRS 5	JRS Pharma	2	2000	2200
JRS 6	JRS Pharma	3	2000	2200
JRS 7	JRS Pharma	2	3000	2200
JRS 8	JRS Pharma	3	3000	2200

Fig. 1. Picture of the Masuko supermass colloider equipment obtained from the manufacturer's internet site. (Source: Masuko Sangyo 2024)

In Aalto University, the Masuko equipment (MKZA10-15; Masuko Sanguo Co., Ltd, Kawaguchi-city, Saitama-pref, Japan) was modified to process wet cellulose and to control was enhanced by automatic, computer-controlled grinding-load adjustment and special feeding pump, and a feeding arrangement that both cools the grit-like fillings by circulating the excess material back to the pump intake/or feeding chamber. Figure 1 presents a picture of Masuko supermass colloider device in its original setup.

Test Standards and Methods

Particle size measurements were conducted for the processed wet samples (dry solids content 10%). Other analyses were carried out for the dry samples prepared though a solvent exchange procedure with fully water miscible low molecular alcohol to avoid hornification or other structural changes that occur with the presence of water during cellulose drying. A solvent exchange procedure was completed with approximately 1.0 g of the sample (calculated as oven dry basis), which was measured into a 50-mL centrifugal tube. The tube was filled with *tert*-butanol, shaken vigorously, and centrifuged at 7500 rpm for 10 min. The liquid fraction was decanted, and the tube was filled again with *tert*-butanol. This procedure was repeated five times. The solvent exchanged cellulose samples were placed at -22 °C for 4 h. Finally, the samples were lyophilized with a freeze dryer (Labconco Freezone 2.5, Kansas City, USA) for 12 h.

The particle size distribution of the samples was measured with a Mastersizer 2000 equipped with a Hydro 2000MU dispersion unit (Malvern Instrument Ltd, Worcestershire, UK). The measurement was conducted as published (Vanhatalo and Dahl 2014). Particle size distribution $d(0.1)$, $d(0.5)$, and $d(0.9)$ values were reported to describe physical particle sizes (μm). All measurements were done in triplicate.

The structural morphology of the samples was observed with scanning electron microscopy (Zeiss Σigma-VP, Jena, Germany) at 3 keV, equipped with an Everhart-

Thornley detector. Prior to imaging, the samples were sputter coated (Emitech K-100X, Lewes, United-Kingdom) with a 5-nm gold-platinum layer to obtain proper conductivity.

Rheological investigations were performed using a strain-controlled rheometer (Physica MCR-300 Anton Paar, Ashland, VA, USA) equipped with 25-mm diameter surface-profiled (serrated) plate-to-plate geometrics. All cellulose hydrogels were measured at 23 °C using a 2-mm measurement gap. A 20 s pre-shear stage was performed at a shear rate of 10 s^{-1}, followed by a settling time of 180 s prior to the amplitude sweep. The amplitude sweep was performed using a constant angular frequency (1 s^{-1}) at increasing strain amplitudes (0.01% to 500%). The moduli value (G' and G'') at a damping factor $\tan(\delta) = 1$ was used to describe the gel strength of the samples, which can also be related to the strength of the spatial network.

To estimate the amount of water retained by the fiber particles, the fiber saturation point (FSP) of the MFCs was determined. FSP measures the water within the cell wall of a saturated fiber and in this study solute exclusion technique with dextran as molecular probe was used (Stone and Scallen 1986). The centrifuged sample solution was measured with a polarimeter (Autopol IV, Rudolph Research, United-Kingdom).

To describe the net value of power used on the fibers during mechanical processing, specific energy consumption, SEC was calculated by Eq. 1 (Lundin *et al.* 2008),

$$SEC = \frac{P_{tot}-P_o}{VC}\left(\frac{kWh}{t}\right) \tag{1}$$

where P_{tot} is total power consumption (kWh), P_{o} is idle power (kWh), V is flow (l/h) and C is concentration of pulp in the water (t/L).

RESULTS AND DISCUSSION

Effect on Particle-Size

Charani *et al.* (2013) suggested that the distribution of differing sizes of the pulp fiber particles in the cellulose hydrogels, such as MFC, generates corresponding differences in the gel strength, such that it can be regarded as an important factor in the rheology of the material suspensions and gels. Figure 2 shows the particle sizes of the grinded samples with the different particle size distributions. The size distributions $d(0.1)$, $d(0.5)$ and $d(0.9)$ are statistical parameters from the cumulative particle size distribution and indicate the size below which 10%, 50% or 90% of all particles are found. The never-dried MCC raw material sizes with distributions $d(0.1)$, $d(0.5)$ and $d(0.9)$ were 15 μm, 50 μm and 140 μm, respectively. The commercial raw material, the JRS Pharma MCC had an average particle size of 65 μm.

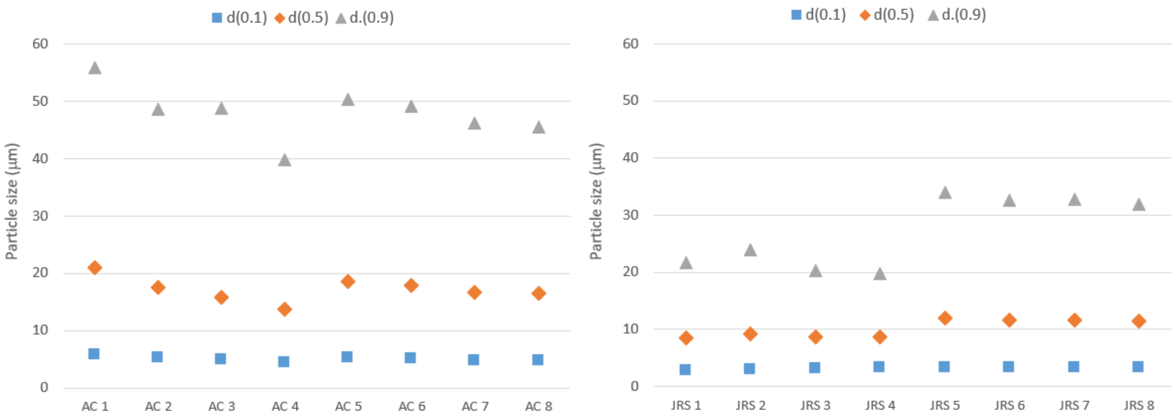

Fig. 2. Particle size values *d*(0.1), *d*(0.5), and *d*(0.9) of the produced cellulose hydrogels

The particle size distribution *d*(0.1), which contains the smallest particles, decreased from 15 µm to about 5 µm with all the never-dried MFC samples. It can be noted that alteration of grinding parameters did not have any great effect on the smallest particles with either raw material. Therefore, it can be concluded that the minimum achieved particle size in MFC production with Masuko was around 5 µm with never-dried MCC raw material and 3 µm with commercial MCC raw material.

With the distribution *d*(0.5), the particle size of the never-dried samples decreased from 50 µm to the range 14 to 20 µm when compared to the size of the same distribution of the never-dried raw material MCC. Furthermore, the particle size of the never-dried MFC samples was decreased notably during the first pass through the grinder when both the power and rotating speed were increased. In contrast, with the ground commercial MFC samples, the particle size did not undergo any major changes with the increase of the grinding intensity or grinding passes. With multiple passes through the grinder, the decreasing behavior was similar with never-dried MFC samples, but the effect was not as great as with the first pass.

Compared with the other distributions, the grinding process had the greatest effect on the largest particles, which are represented by the particle size distribution *d*(0.9). Especially with the first pass never-dried samples, where the particle size decreased remarkably from 140 µm to 40-55 µm, even with multiple passes through the grinder. The size of the largest particles, *d*(0,9) stayed within 20 µm with commercial MFC samples during the first pass. Surprisingly, the size of this distribution increased from 20 µm to more than 30 µm with additional passes through the grinder. This development is most likely due to the formation of particle agglomerates and flocs, which can be explained by the MCC's drying history. When MCC is dried, a high density of hydrogen bonds in a pattern are formed between the fibrils which re-swelling or rehydration does not replace, making it difficult to separate agglomerates (Iwamoto *et al*. 2008). Furthermore, the higher feed consistencies induce fiber flocculation due to the relatively high fiber aspect ratio of MFC fiber network (Ankerfors 2012).

When considering the grinding parameters' effects on the different raw materials, the produced never-dried MFC and the commercial MFC demonstrate relatively different behavior. With never-dried samples, this raw material responded in a highly noticeable manner to the changes made with the grinding parameters. This effect was more apparent with larger particles, as might be expected. While the particle size drop was very significant with respect to the never-dried MFC samples, with commercial MFC samples, the increase in grinding power (load) from 2000 to 3000 W caused only minor decrease in the larger particle size distributions with the first pass through the grinder. This decrease was even less visible with the second and third pass with commercial MFC samples, while it was still very visible with never-dried samples. With the first pass through the grinder, the particle size of the never-dried MFC samples in distribution *d*(0.9) and distribution *d*(0.5) decreased around 10 μm and 5 μm, and the corresponding change being -19% and -31%, respectively, with increased grinding power. With additional passes through the grinder, the equivalent reduced values with distributions *d*(0.9) and *d*(0.5) were 5 μm, -8 % and 3 μm, -10 %, respectively.

When considering rotation speed, representing the shear forces, with the increase from 1700 to 2200 rpm, the effect to the never-dried samples was almost linear with power increase. With first pass, the particle size of the never-dried MFC samples in distribution d(0.9) decreased *circa* 7 μm and with distribution *d*(0.5) 2.5 μm, and the corresponding percentage being -19% and -17%, respectively, with the increased grinding load.

The decrease in the particle size was clearer with larger rotation speed (2200 rpm). The change of rotation speed seemed to have no effect on the particle size with larger grinding power (3000 W). Second pass through the grinder significantly increased the largest particle size distribution, which is most likely due to the formation of agglomerates. Third pass did not seem to have any notable effect on any of the particle size distributions. Therefore, it can be concluded that the greatest effect on particle sizes was achieved on the first pass.

Fiber Saturation Point

Figure 3 represents the measured FSP values of the produced MFC samples. FSP corresponds to the amount of water contained within the water-saturated cell wall. Nakai *et al.* (1977) found that the water sorption capacity is strongly dependent on the specific kind of MCC, on its fine physiochemical properties and on the conditions of chemical and mechanical pretreatments adopted.

The FSP values were much higher with never-dried MFC samples than the ones produced with commercial dried MCC. This can be traced to the hornification effect that happened during the drying of the commercial MCC raw material. Hornified fibers have reduced swelling capacity that can be seen as a decrease in FSP values which has been recognized by several previous studies (Park *et al.* 2006; Hubbe *et al.* 2007; Chen *et al.* 2011; Idström *et al.* 2013). The hornification mechanism is described as the formation of coalesced microfibrils by irreversible H-bonds during drying and rewetting by Iwamoto *et al.* (2008). With the grinded MFC samples from commercial MCC, the FSP values did not show any clear trends. However, it seems that small increases in FSP values can be obtained by adjusting the grinding parameters. At higher power levels a minor decrease in FSP was observed.

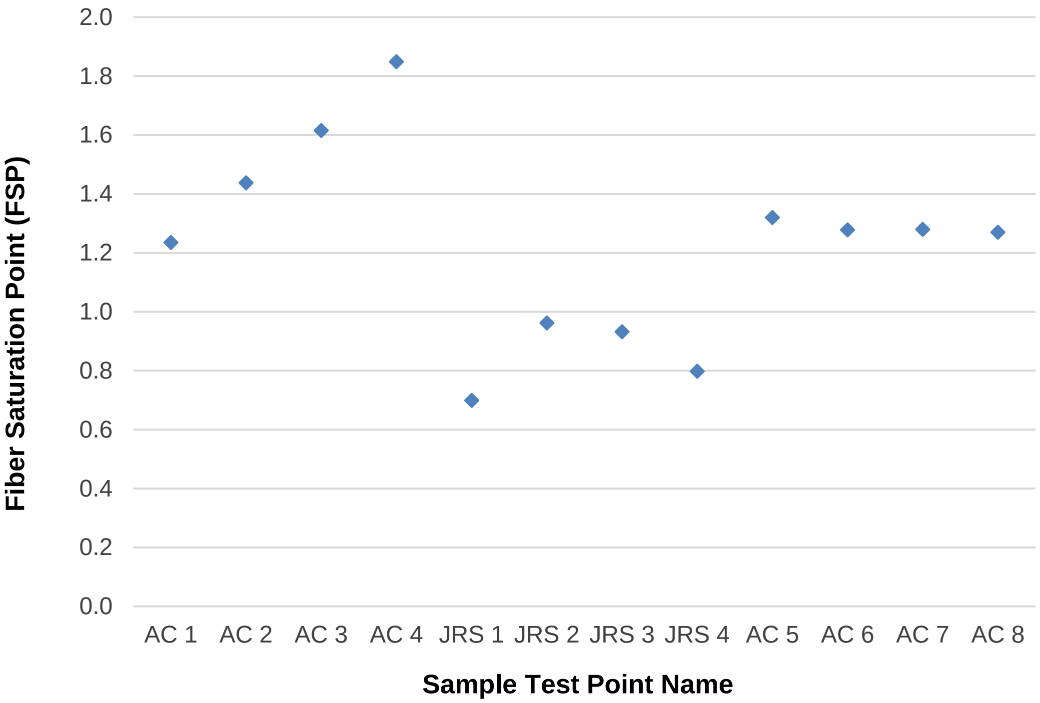

Fig. 3. The fiber saturation point (FSP) values for produced MFC samples

In the first pass through the grinder, the FSP values of never-dried samples grew *circa* 30% with increasing the grinding power and *circa* 15% with the increase of the rotation rate of the grinder. Here it seems that the increase in grinding power increased the FSP value half more than the increase of rotation rate. With the increase of both the grinding parameters, almost 34% increase in FSP value was achieved with never-dried samples. When compared to the FSP values of the commercial raw material samples, *circa* 30% increase was achieved, with similar grinding parameters.

With the first pass through the grinder, the increase in grinding power and grinder's rotation speed gradually increased the FSP values of never-dried samples. This trend correlated with the decrease of the particle sizes with never-dried MFC samples. The increase in FSP appears to have been the result of the greater swelling capacity produced by the greater fiber fibrillation created during the grinding process. Apparently, the ability of the MFC samples to hold water increased with the growing specific surface area (fiber fibrillation) and with the decreasing particle sizes. However, the increase in grinding passes did not increase the FSP values of never-dried MFC samples any more. It seems that the optimal grinding effect on the fiber fibrillation was achieved with the first grinding pass, and multiple passes will instead break down the achieved fibrillation of the MFC particles.

Rheological Properties

Rheology reflects the behavior of the MFC sample suspensions during further processing and storage. The viscoelastic properties are used to monitor the state of dispersion, the binding behavior of the cellulose surface for water, and the forming of the gel-like structure. Alterations in the degree of particle entanglement, agglomeration, and/or flocculation in the network structure, are shown as a change of the mechanical and viscoelastic properties of the suspension, including gelation (Dimic-Misic *et al*. 2018). The gelation properties of the produced MFC hydrogels samples were studied with moduli values *G*' and *G*", which are a measure of the elastic and viscous components, respectively. These modulus values describe the strength and behavior of the MFC hydrogels, and they give indication of how fluid-like the produced material is. Viscoelastic storage, *G*' and loss modulus, *G*" are illustrated in Figs. 4 and 5 as functions of the shear strain of the manufactured MFC samples based on the results from strain sweep tests. In the gel state the elastic behavior dominates, and *G*' is higher than *G*" (Pääkkö *et al.* 2007). As can be noted from Figs. 5 and 6, all the investigated MFC samples showed a gel-like behavior.

Rheological properties of MFC depend strongly on the fibril dimensions, manufacturing procedure, and the raw materials used (Saito *et al.* 2007; Iwamoto *et al*. 2008). With weakly bonded fiber network, the network falls apart easily when exposed to increased shear rate, and individual elements start to flow. The large aspect ratio of the MFC particles encourages the contact among fibers and has a strong effect on rheological behavior of the MFC gel (Littunen *et al*. 2011). In general, the more entangled fiber network, the stronger the MFC hydrogel.

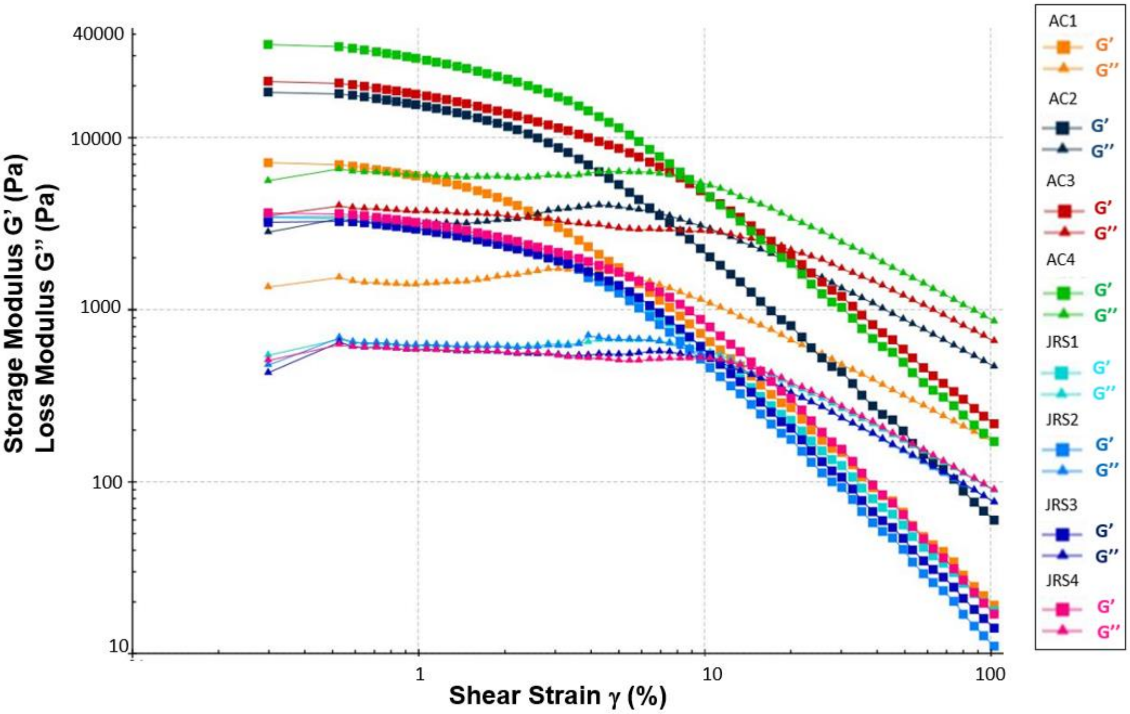

Fig. 4. The storage modulus, *G*' (squared dots) and the loss modulus, *G*'' (triangular dots) as a function of the shear strain of the manufactured MFC samples after one pass through the Masuko grinder.

The linear viscoelastic region of the MFC samples is the part of the curve where *G*' remains constant as the more energy is applied to the sample. As the amplitude intensifies, the structure of the MFC begins to break down. The point of the breakdown is known as critical strain. It defines the end of the linear viscoelastic region and thus provides information on the nature of the internal structure of MFC material. As can be seen from *G*' curves from Figs. 4 and 5, all the manufactured MFC samples had a short linear viscoelastic region, after which the MFC structure began to collapse.

With the first refining pass, the *G*’ of the never-dried samples grew with the intensity of the grinding. This development reflects the increased surface area and the greater number of thinner fibrils with more trapping water, leading to a strong homogeneous gel-like structure of the MFC suspension. The increase in the rotation rate increased the storage modulus clearly, but the increase in the grinding power made the modulus grow even more. Refining parameters had huge effects here. Enhanced strength of the gel network by the increased fiber fibrillation during grinding was reflected visibly in the higher elastic modulus values. All the MFC sample curves showed the same trend, except the sample AC3 (3000 W, 1700 rpm), which was not wearing off as fast as the others. This may be the optimal grinding point in relation to MFC’s rheological properties. As can be expected, the *G*’ of the least refined sample AC1, wears off more drastically than the others, signifying the weakest structure of MFC.

The results acquired by Dimic-Misic *et al.* (2018) and Dong *et al.* (2018) are important reference points here, since those researchers used the same raw material in the MFC production with HPH: the never-dried MCC made with the AaltoCell^{TM} procedure. These findings are in good accordance with this study. All the researched MFC hydrogel samples showed a constant modulus until the stress passed the yield point of the MFC and decreased remarkably. The values of *G*” were typically a 10-fold less to the *G*’ values for each hydrogel sample. Dimic-Misic *et al.* (2018) explained that this difference in the modulae magnitudes reflects the combination of high colloidal stability derived from mutual charge repellence in addition to the combination of the surface adsorbed and trapped water structure.

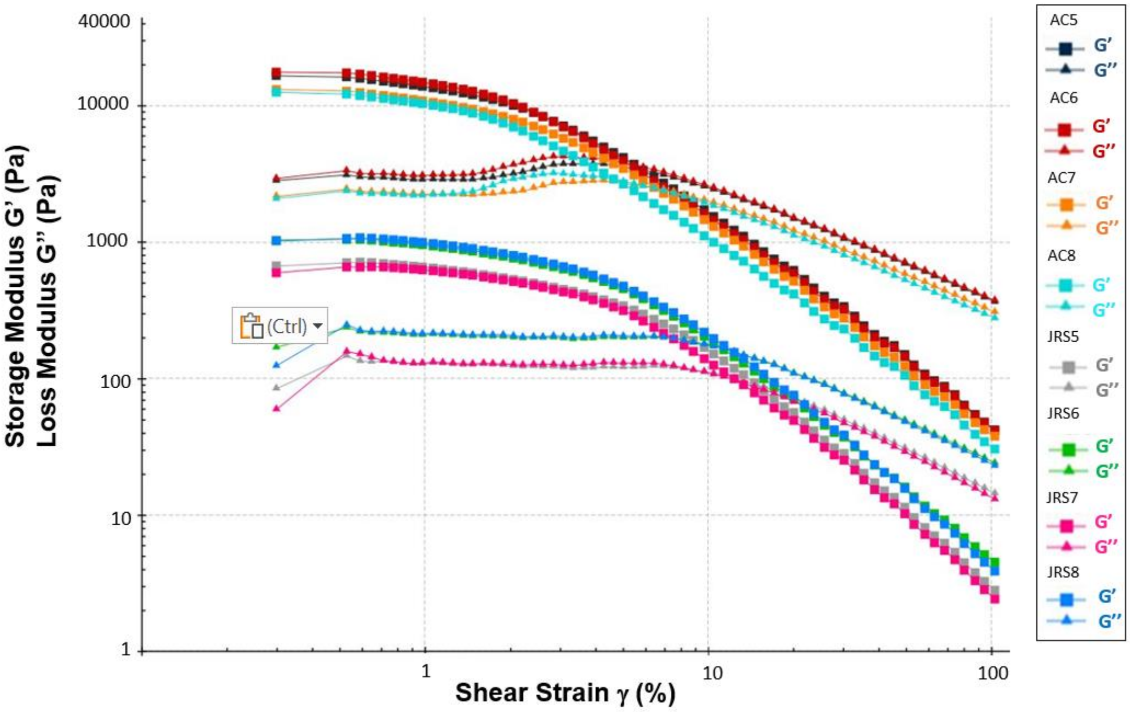

Fig. 5. The storage modulus, *G*’ (squared dots) and the loss modulus, *G*’’ (triangular dots) as a function of the shear strain of the manufactured MFC samples after second and third pass through the Masuko grinder.

With the MFC samples made from commercial MCC samples, the *G*' values were considerably smaller than those of the never-dried samples already with the first pass through the grinder, almost 10 times smaller. As it was shown with the other fiber properties' results, also here the grinding parameters clearly had much less effect on the dried MCC. The modulus values showed a small increase with the most intensified grinding. After the shear stain of 6%, the *G*' of the commercial samples started to correlate with the least ground never-dried sample. The loss modulus, *G*" of all commercial samples was a bit weaker with stronger grinding, but all in all the differences were small. The differences in MFC sample gel strengths and behavior were probably linked to the drying history of the two MCC raw materials that had gone through different structural changes in their cellulose matrices in their production processes. The never-dried MCC structure could provide stronger MFC gel strengths, likely due to a higher degree of never-collapsed but fibrillated structures at different length scales, as noticed also by Vanhatalo *et al.* (2016). The present study supports the assumption made in studies by Kontturi and Vuorinen (2009) that drying induces irreversible aggregations of fibrillar structures in cellulose.

The storage modulus of never-dried samples after the second and third passes did show a minor difference in this point with the intensity of the grinding. An increase in the grinding power will lead to a slight decrease in the modulus. On the other hand, it seems that too strong refining will weaken the produced MFC, as seen in the FSP results. All the sample *G*' curves exhibited the same trend, also corresponding with the FSP results. With the additional passes through the grinder, the *G*' values of the commercial MFC samples were much smaller than those of the never-dried samples', more than 10 times smaller. However, the third pass seemed to have a small increase in the modulus values, more clearly than with never-dried samples. The second and third pass samples had almost identical curves (as are their particle sizes).

The loss modulus with commercial samples showed similar behavior as the storage modulus with multiple passes. The third pass increased the loss modulus values like the storage modulus. With the never-dried samples the behavior with increasing passes was less clear, since the curves exhibited different behavior compared to the commercial ones. The samples grinded with smaller load seemed to have higher loss modulus. The increase in the grinding load led to a small decrease in the modulus.

It can be noted that the FSP values (shown in Fig. 3) increased along with the strength of the produced MFC cellulose hydrogels samples. Stronger MFC gels were formed most probably due to the formation of new internal surface area and porosity created by the increased fiber fibrillation. Dimic-Misic *et al.* (2018) suggested that the stronger gel-like behavior of cellulose gels is produced by the more pronounced hydrogen bonding within the cellulose particle suspension due to the high surface area in the dispersed wet state. Vanhatalo (2017) proposed that the increased modulus values and water holding capacity values are developed probably from the AaltoCell™-type MCC's never-dried and thus more porous structures. This is also supported by Ioelovich and Leykin (2008), who also noticed that the drying of MCC causes the irreversible closing of the particles' internal pores. Dong *et al.* (2018) stated that the greater gel forming ability of the mechanically treated never-dried MCC particles compared with the dried commercially grade MCC is due to the opened fibrillar structure and higher elasticity of the never-dried material.

Refining Efficiency and Energy Consumption

The specific energy consumption (SEC) of the grinded MFC gel samples is presented in Table 2 and in Fig. 6. The specific energy consumptions of the manufactured never-dried MFC gels are considerably higher than those of the MFC samples made from the dried commercial MCC. However, it seems that the gentlest grinding (2000 W or 1700 rpm) of the never-dried AaltoCell^{TM} MCC consumed less energy compared to the commercial dried MCC with all the refining passes. With all the other refining parameter combinations, the grinding of never-dried MCC needed more refining energy than the grinding of the dried commercial MCC. Nevertheless, this can be seen straight in the MFC gel properties that were significantly superior with the never-dried MFC samples in relation to fiber swelling and rheology than with the MFC samples made from the dried commercial MCC. Due to these factors, it can be stated that the refining action and the consumed energy is transferred more profoundly into the never dried structure of the AaltoCell^{TM} MCC.

Table 2. Specific Energy Consumptions (SEC) of the MFCs with the Used Grinding Parameters

Raw Material	Grinding Load	Rotation Rate	SEC	SEC	SEC
			1.Pass	2. Pass	3.Pass
(MCC type)	(W)	(rpm)	(kWh/kgOD)	(kWh/kgOD)	(kWh/kgOD)
AaltoCell	2000	1700	0,087	-	-
AaltoCell	3000	1700	1,734	-	-
AaltoCell	2000	2200	0,941	1,031	1,113
AaltoCell	3000	2200	1,541	1,665	1,762
JRS Pharma	2000	1700	0,712	-	-
JRS Pharma	3000	1700	1,114	-	-
JRS Pharma	2000	2200	0,538	0,622	0,674
JRS Pharma	3000	2200	0,883	1,006	1,099

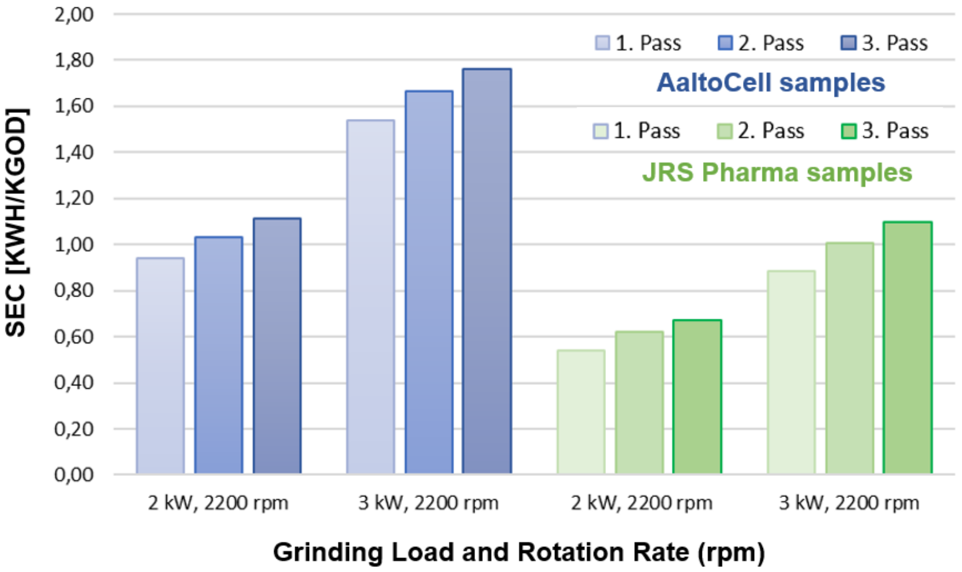

Fig. 6. The Specific Energy Consumption, SEC (kWh/kgOD) of the manufactured MFC sample test points, the darker color indicating the more profound refining

Fiber saturation point, the measure of the internal fibrillation of fiber, is one of the indicators of the refining degree. It can be used as the measure of the refining effect. When FSP is plotted as the function of the SEC, as illustrated in Fig. 7, a clear correlation can be found in the increase in both the values with never-dried MFC samples that had been passed the grinder the first time. When excluding the least grinded test point sample, the same correlation can be seen with the MFC samples manufactured from the commercial dried MCC. Furthermore, when comparing these two raw materials, it can be noted that with the never-dried MCC, greater FSP values can be obtained with the same energy consumption, when compared to the MFC made from the dried commercial MCC. This suggests that less energy could be used when using the never-dried MCC as a raw material in the mechanical MFC production process. Dimic-Misic *et al.* (2018) observed that never-dried MCC's fibril-like structure enables the mechanical work to be applied directly to the particles as a function of specific surface. Consequently, using unnecessary energy for overcoming the mechanical elastic structure associated with entangled and retained fibers can be avoided. Additionally, Liimatainen *et al.* (2014) produced MFC by using HPH and suggested that micro-fibril production with hornified fibers involves higher energy.

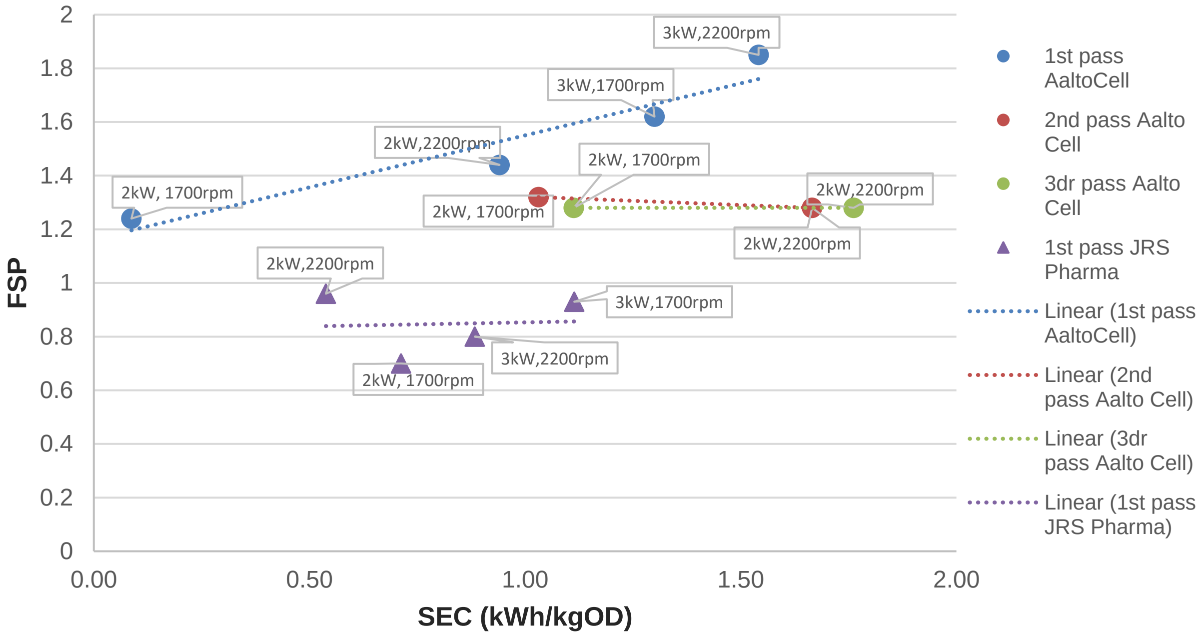

Fig. 7. The FSP as a function of the SEC of the manufactured MFC samples

The particle size distribution (0,9) is plotted as the function of the SEC in Fig. 8. With the same amount of energy, a greater impact was achieved on the never-dried AaltoCell^{TM} MFC product than on the MFC samples made from dried raw material. On the other hand, the particle size of the never-dried MFC product was larger before processing. Hence, the impact was greater during the initial grinding. During the second and third pass-through, the energy was insufficient to break down the flocs. The smallest size of the never-dried MFC was achieved with the first pass-through. It was previously observed that the never-dried MFC absorbed energy more efficiently. Furthermore, from the graphs, it can be noted that the effects of product processing were essentially established during the first processing cycle, where the induced change was the greatest. The second or third processing cycle may even deteriorate the product's properties, possibly due to the phenomenon of agglomeration. Importantly, these results seem to correlate well with the FSP results.

When comparing the specific energy consumption results with the other MFC studies, the SEC values obtained in this study appear quite low. For comparison, Josset *et al.* (2014) made MFC experiments and reported values for energy consumption of the grinder after ten passes 5.25 kWh/kg for ECF pulp, which implies approximately 0.7 kWh/kg per cycle. Their results also indicated that the most significant changes in the produced MFC were achieved during the first two cycles. Moreover, other studies focusing on reducing energy consumption, such as Zhu *et al.* (2012) and Lindström *et al.* (2012), have reported an approximate energy consumption of 0.76 kWh/kg with TEMPO and endoglucanase treated pulp. However, it must be noted that all the compared energy consumptions are not based to the same MFC properties and use different raw material than in this study and are therefore only indicative and cannot be straightly compared with one another.

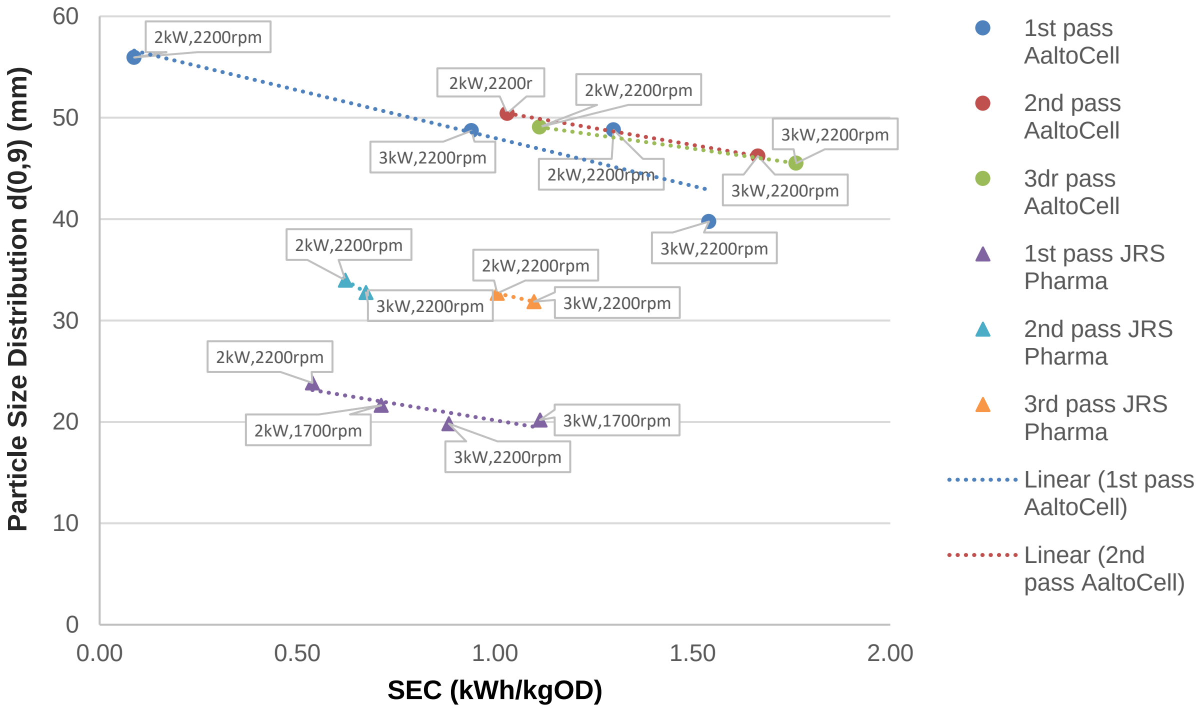

Fig. 8. The particle size distribution d(0,9) as a function of the SEC of the manufactured MFC samples

Here in the present study, the energy consumption values fell within a range of typical values, suggesting that the major impact of the grinding is produced in the first processing, and that the result from the first processing step can be drastically modified depending on the parameters of the grinding and the feedstock. With additional passes through the grinder, no increase in FSP or decreasing of the particle size were obtained with the consumed greater refining energy, indicating that no further refining effect could be gained with further grinding passes. This is most likely caused by the recreation of particle flocs/ agglomeration and/or peeling off the already obtained external fibrillation from the particle surfaces due to excess grinding. The results gained by Josset *et al*. (2014) also indicated that the most significant changes in the produced MFC were achieved during the first two cycles of grinding.

Structural Morphology

The morphology of the MFC samples AC3 and AC4 as well as their raw material never-dried AaltoCell^{TM} MCC was captured in SEM micrographs. The samples AC3 and AC4 were selected to show the SEM imaging, since they produced the most superior MFC properties. By the visual assessment of SEM-images, presented in Fig. 9, the changed cellulose fiber architecture after the mechanical MFC production can be identified. The never-dried raw material MCC shows clear individual fiber-like architecture, which appears as bundles of needle like cellulose microcrystals with smooth and intact fibril surfaces. The micrographs of the produced MFC samples verify that the mechanical grinding process resulted in partial defibrillation of the cell wall, thus producing cellulose microparticles having fibrillary surfaces. These particles appear to be bundles of partially damaged microfibrils. They display significant external fibrillation without complete removal of fibrils. The ground MFC particles form a tight network by the entanglement of micro and nanofibrils which lead to an increase in accessible cellulose surface area.

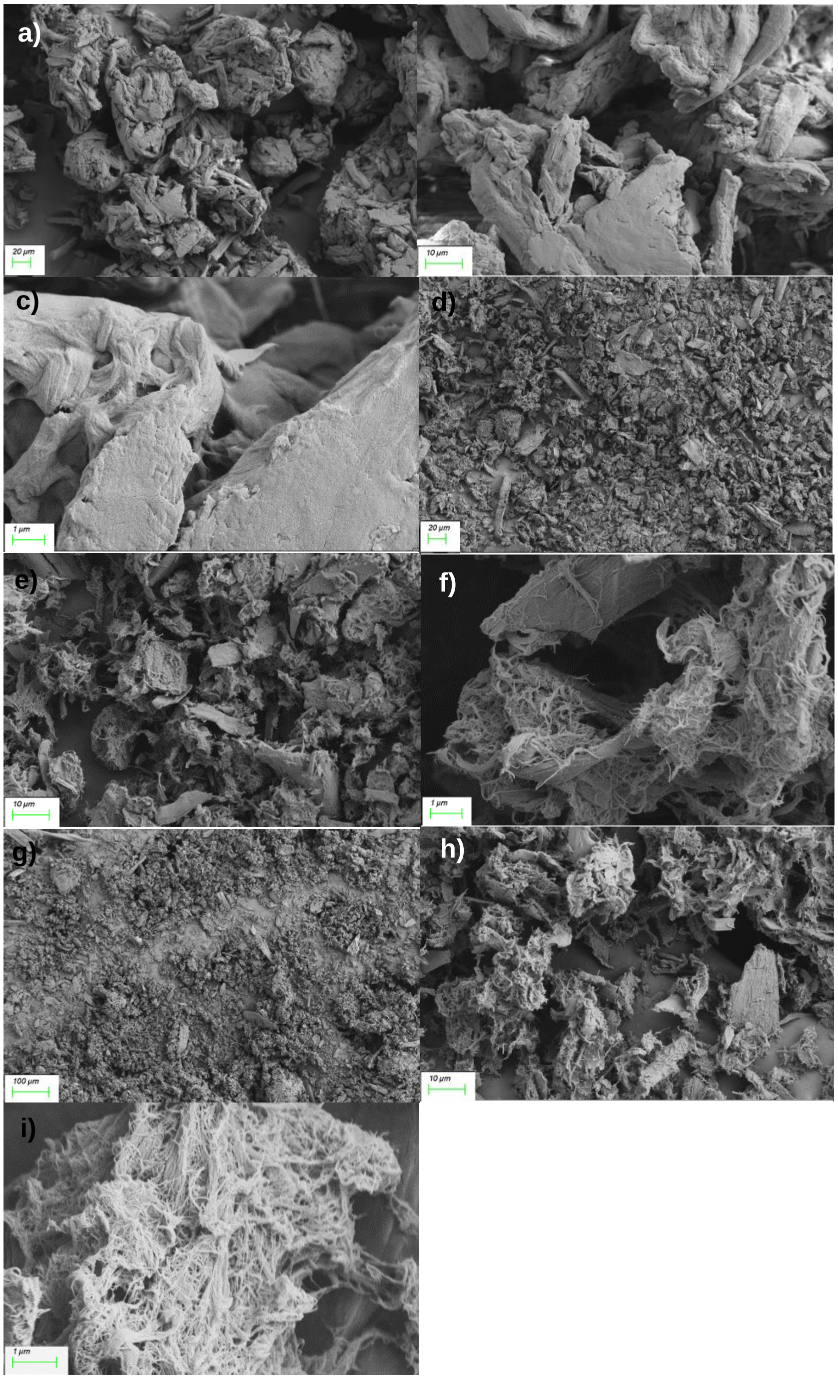

Fig. 9. SEM micrographs with three different magnifications of the never-dried MCC raw material (pictures **a, b,** and **c)**, the produced MFC samples AC3 (pictures **d, e,** and **f**) and AC4 (pictures **g, h,** and **i**).

Confirming the particle size distributions measurements, SEM images of both manufactured MFC samples AC3 and AC4 showed noticeably smaller particles than the raw material MCC. This is the direct result of the dimensional reduction of the fibers by cutting during the grinding. Moreover, the micrographs endorse visually minor but nonetheless considerable differences between the two produced MFC samples. The less ground sample AC3 shows slightly less entangled and fewer externally fibrillated structures than the sample AC4. As the refining intensifies, an increase in surface area occurs due to greater fibrillation, as can be seen from Figs. 9h and 9i. This most probably manifested itself with different rheological behavior that was seen in the storage and loss modulus results, where the sample AC4 showed superior modulus values in comparison to the sample AC3.

In conclusion, it can be confirmed from the SEM-imaging that the mechanical treatment with Masuko grinder was able to fibrillate the MCC particles partly, resulting in micron-sized particles with nanofibrillar surfaces. The grinding caused partial opening of the nano-fibrillary structure of MCC particles and entanglement of individual particles that led to formation of an elastic network of MFC with increased FSP values and notable rheological properties.

CONCLUSIONS

1. The research focused on the refining effects of Masuko friction grinder on the properties of never-dried microcrystalline cellulose (MCC) compared to the traditional commercially available dried MCC. It was observed that the grinding parameters had a greater and more profound impact on the never-dried MCC compared to the commercial MCC, which is likely attributable to the hornification effect that the commercial raw material underwent during its drying.
2. Based on the present results, the fiber saturation point (FSP) and the elastic modulus values were markedly higher for the never-dried microfibrillated cellulose (MFC) samples, implying the greater achieved fibrillation of the never-dried fiber structure during the grinding process. The never-dried MCC structure provided stronger MFC gel that was able to bind more water than the MFC manufactured from dried MCC, likely due to a higher degree of never-collapsed but fibrillated structures at different length scales.
3. The most significant reduction in particle sizes as well as the greatest increase in FSP value and rheological properties were achieved during the initial pass through the Masuko grinder. The obtained results also implied that subsequent grinding passes may be unnecessary and potentially weaken the properties of the produced MFC – possibly due to the formation of flocs and agglomerates.
4. The specific energy consumption results of the MFC production also indicated that less energy was consumed in the case of the never-dried MCC to achieve the same degree of fibrillation since the grinding energy transfers more efficiently into the never-dried MCC structure.
5. It was possible to refine the MCC slurry into MFC with the higher consistency of 10% without any problems and still achieve high external fiber fibrillation.
6. The never-dried MCC showed a strong potential as a raw material for cost-effective MFC production due to its lower refining energy consumption and reduced transportation costs made possible by the higher processing consistency.

ACKNOWLEDGMENTS

The authors are grateful for all the support given by the staff of the Department of Bioproducts and Biosystems, Aalto University School of Chemical Technology.

REFERENCES CITED

Ankerfors, M. (2012). *Microfibrillated Cellulose: Energy-efficient Preparation Techniques and Key Properties*, Licentiate Thesis, KTH Royal Institute of Technology, Sweden.

Ardanuy, M., Claramunt, J., Arévalo, R., Parés, F., Aracri, E., and Vidal, T. (2012). "Nanofibrillated cellulose (NFC) as a potential reinforcement for high performance cement mortar composites," *BioResources* 7(3), 883-3894. DOI: 10.15376/biores.7.3.3883-3894

Charani, P. R., Dehghani-Firouzabadi, M., Afra, E., and Shakeri, A. (2013). "Rheological characterization of high concentrated MFC gel from kenaf unbleached pulp," *Cellulose* 20, 727-740. DOI: 10.1007/s10570-013-9862-1

Dimic-Misic, K., Vanhatalo, K., Dahl, O., and Gane, P. (2018). "Rheological properties comparison of aqueous dispersed nanocellulose derived from a novel pathway-produced microcrystalline cellulose or by conventional methods," *Applied Rheology* 28(6), article ID 64474. DOI: 10.3933/ApplRheol-28-64474

Dimic-Misic, K., Maloney, T., and Gane, P. (2018). "Effect of fibril length, aspect ratio and surface charge on ultralow shear-induced structuring in micro and nanofibrillated cellulose aqueous suspensions," *Cellulose* 25, 117-136. DOI: 10.1007/s10570-017-1584-3

Dong, Y., Paukkonen, H., Fang, W., Kontturi, E., Laaksonen, T., and Laaksonen, P. (2018). "Entangled and colloidally stable microcrystalline cellulose matrices in controlled drug release," *International Journal of Pharmaceutics* 548(1), 113-119. DOI: 10.1016/j.ijpharm.2018.06.022

Guezennec, C. (2012). *Development of New Packing Materials-based on Micro- and Nano-fibrillated Cellulose*, Doctoral Thesis, Grenoble University, Grenoble, France.

Henriksson, M., Henriksson, G., Berglund, L. A., and Lindström, T. (2007). "An environmentally friendly method for enzyme-assisted preparation of microfibrillated cellulose (MFC) nanofibers," *European Polymer Journal* 43(8), 3434-3441.

Ioelovich, M., and Leykin, A. (2008). "Study of solid-liquid interface in water dispersions of microcrystalline celluloses," *Composite Interfaces* 15(7-9), 771-779.

Iwamoto, S., Abe, K., and Yano, H. (2008). "The effect of hemicelluloses on wood pulp nanofibrillation and nanofiber network characteristics," *Biomacromolecules* 9(3), 1022-1026. DOI: 10.1021/bm701157n

Josset, S., Orsolini, P., Siqueira, G., Tejado, A., Tingaut, P., and Zimmermann, T. (2014). "Energy consumption of the nanofibrillation of bleached pulp, wheat straw and recycled newspaper through a grinding process," *Nordic Pulp & Paper Research Journal* 29(1), 167-175.

Kondo, T., Kose, R., Naito, H., and Kasai, W. (2014). "Aqueous counter collision using paired water jets as a novel means of preparing bio-nanofibers," *Carbohydrate Polymers* 112, 284-290. DOI: 10.1016/j.carbpol.2014.05.064

Kontturi, E, and Vuorinen, T. (2009). “Indirect evidence of supramolecular changes within cellulose microfibrils of chemical pulp fibers upon drying,” *Cellulose* 16, 65-74.

Lahtinen, P., Liukkonen, S., Pere, J., Sneck, A., and Kangas, H. (2014). “A comparative study of fibrillated fibers from different mechanical and chemical pulps,” *BioResources* 9(2), 2115-2127. DOI: 10.15376/biores.9.2.2115-2127

Lengowski, E. C., Bolzon de Muñiz, G. I., Sulado de Andrade, A., Leonardo Coelho, S., and Nisgoski S. (2018). “Morphological, physical and thermal characterization of microfibrillated cellulose,” *Revista Árvore* 42(1), article ID e420113. DOI: 10.1590/1806-90882018000100013

Liimatainen, H., Kekäläinen, K., Illikainen, M., Maloney, T., and Niinimaki, J. (2014). “The role of hornification in the disintegration behaviour of TEMPO-oxidized bleached hardwood fibres in a high-shear homogenizer,” *Cellulose* 21(3), 1163-1174. DOI: 10.1007/s10570-014-0210-x

Lindström, M. E., Söderberg, D., and Henriksson, G. (2012). “Single-step method for production of nano pulp by acceleration and disintegration of raw material,” World patent No. WO2012/115590.

Littunen, K., Hippi, U., Johansson, L.-S., Österberg, M., Tammelin, T., Laine, J., and Seppälä, J. (2011). “Free radical graft copolymerization of nanofibrillated cellulose with acrylic monomers,” *Carbohydrate Polymers* 84(3), 1039-1047. DOI: 10.1016/j.carbpol.2010.12.064

Lundin, T., Batchelor, W., and Fardim, P. (2008). “Fiber trapping in low-consistency refining: New parameters to describe the refining process,” *TAPPI J* 7(7), 15-21.

Nakai, Y., Fukuoka, E., Nakajima, S., and Hasegawa, J. (1977). “Crystallinity and physical characteristics of microcrystalline cellulose,” *Chemical and Pharmaceutical Bulletin* 25(1), 96-101.

Manninen, M., Kajanto, I., Happonen, J., and Paltakari, J. (2011). “The effect of microfibrillated cellulose addition on drying shrinkage and dimensional stability of wood-free paper,” *Nordic Pulp & Paper Research Journal* 26, 297-305. DOI: 10.3183/npprj-2011-26-03-p297-305

Moon, R. J., Martini, A., Nairn, J., Simonsen, J., and Youngblood, J. (2011). “Cellulose nanomaterials review: Structure, properties and nanocomposites,” *Chemical Society Reviews* 40, 3941-3994. DOI: 10.1039/C0CS00108B

Pääkkö, M., Ankerfors, M., Kosonen, H., Nykänen, A., Ahola, S., Österberg, M., Ruokolainen, J., Laine, J., Larsson, P. T., Ilkkala, O., *et al.* (2007). “Enzymatic hydrolysis combined with mechanical shearing and high-pressure homogenization for nanoscale cellulose fibrils and strong gels,” *Biomacromolecules* 8(6), 1934-1941. DOI: 10.1021/bm061215p

Saito, T., and Isogai, A. (2004). “TEMPO-mediated oxidation of native cellulose. The effect of oxidation conditions on chemical and crystal structures of the water-insoluble fractions,” *Biomacromolecules* 5(5), 1983-1989.

Saito, T., Kimura, S., Nishiyama, Y., and Isogai, A. (2007). “Cellulose nanofibers prepared by TEMPO-mediated oxidation of native cellulose,” *Biomacromolecules* 8(8), 2485-2491. DOI: 10.1021/bm0703970

Siró, I., and Plackett, D. (2010). “Microfibrillated cellulose and new nanocomposite materials: A review,” *Cellulose* 17, 459-494. DOI: 10.1007/s10570-010-9405-y

Spence, K. L., Venditti, R. A., Rojas, O. J., Habibi, Y., and Pawlak, J. J. (2010). "The effect of chemical composition on microfibrillar cellulose films from wood pulps: Water interactions and physical properties for packaging applications," *Cellulose* 17, 835-848.

Taheri, H., and Samyn, P. (2016). "Effect of homogenization (microfluidization) process parameters in mechanical production of micro- and nanofibrillated cellulose on its rheological and morphological properties," *Cellulose* 23, 1221-1238. DOI: 10.1007/s10570-016-0866-5

Taniguchi, T., and Okamura K. (1998). "New films produced from microfibrillated natural fibres," *Polymer International* 47(3), 291-294.

Turbak, A. F., Snyder, F. W., and Sandberg, K. R. (1983). "Microfibrillated cellulose, a new cellulose product: properties, uses, and commercial potential," in: *Journal of Applied Polymer Science, Applied Polymer Symposium*, John Wiley & Sons Inc, Syracuse, NY, USA, pp. 815-828.

Uetani, K., and Yano, H. (2011). "Nanofibrillation of wood pulp using a high-speed blender," *Biomacromolecules* 12(2), 348-353.

Vanhatalo, K., and Dahl, O. (2014). "Effect of mild acid hydrolysis parameters on properties of microcrystalline cellulose," *BioResources* 9(3), 4729-4740. DOI: 10.15376/biores.9.3.4729-4740

Vanhatalo, K., Lundin, T., Koskimäki, A., Lillandt, M., and Dahl, O. (2016). "Microcrystalline cellulose property–structure effects in high-pressure fluidization: Microfibril characteristics," *Journal of Materials Science* 51(12), 6019-6034. DOI: 10.1007/s10853-016-9907-6

Vanhatalo, K. (2017). *A New Manufacturing Process for Microcrystalline Cellulose (MCC)*, Doctoral Thesis, Aalto University, Espoo, Finland.

Wang, X. (2006). *Improving the Papermaking Properties of Kraft Pulp by Controlling Hornification and Internal Fibrillation*, Doctoral Thesis, Helsinki University of Technology, Espoo, Finland.

Zhang, L., Tsuzuki, T., and Wang, X. (2015). "Preparation of cellulose nanofiber from softwood pulp by ball milling," *Cellulose* 22, 1729-1741. DOI: 10.1007/s10570-015-0582-6

Zhu, H., Helander, M., Moser, C., Stahlkranz, A., Söderberg, D., Henriksson, G., and Lindström, M. (2012). "A novel nanocellulose preparation method and size fraction by cross flow ultra-filtration," *Current Organic Chemistry* 16(16), 1871-1875.

Article submitted: June 16, 2024; Peer review completed: July 31, 2024; Revised version received: September 16, 2024; Accepted: September 16, 2024; Published: October 22, 2024.
DOI: 10.15376/biores.19.4.9375-9395